

Electronic Supplementary Information for Nanoscale

Excitation and Tuning of Fano-like cavity plasmon resonances in dielectric-metal core-shell resonators

Ping Gu,¹ Mingjie Wan,¹ Wenyang Wu,¹ Zhuo Chen,^{1,2,*} and Zhenlin Wang^{1,2,*}

¹*School of Physics and National Laboratory of Solid State Microstructures, Nanjing University, Nanjing 210093, China*

²*Collaborative Innovation Center of Advanced Microstructures, Nanjing University, Nanjing 210093, China*

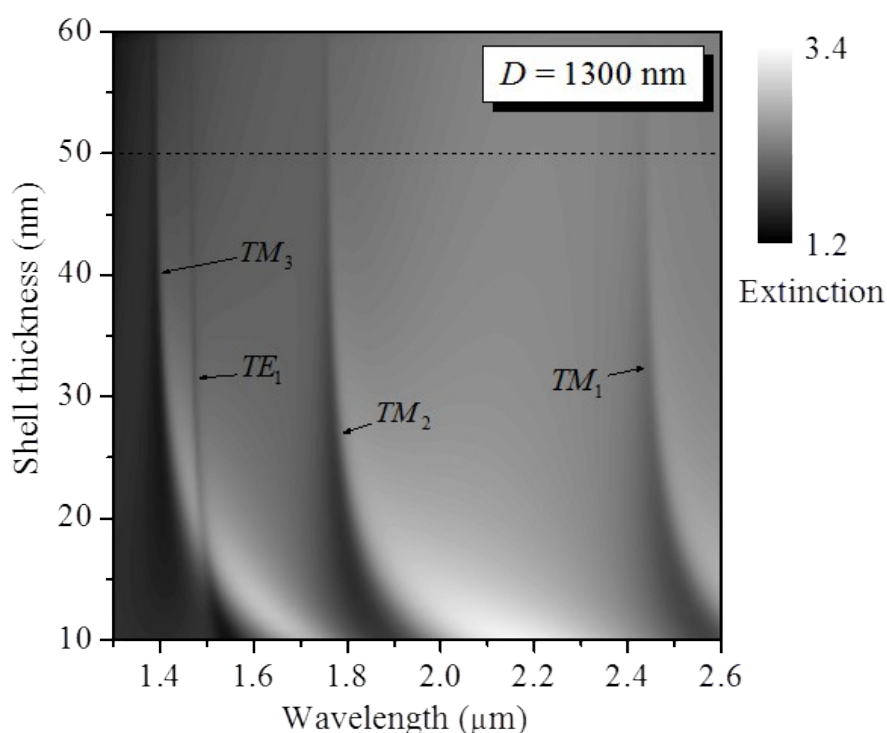


Fig. SI-1 The extinction spectra as both functions of the shell thickness and the wavelength for polystyrene-Ag core-shell resonators with a core-diameter of $D = 1300$ nm, which are calculated using the three-dimensional finite-element-method (FEM) software COMSOL Multiphysics. It is seen that with increasing the shell thickness a resonance blue-shift is observed, which could be attributed to a gradual phase shift upon increased confinement of the fields inside the metal shells. As the shell thickness extends beyond the optical skin depth of silver (~ 30 nm), the increased field confinement saturates, and correspondingly the resonance shift converges.

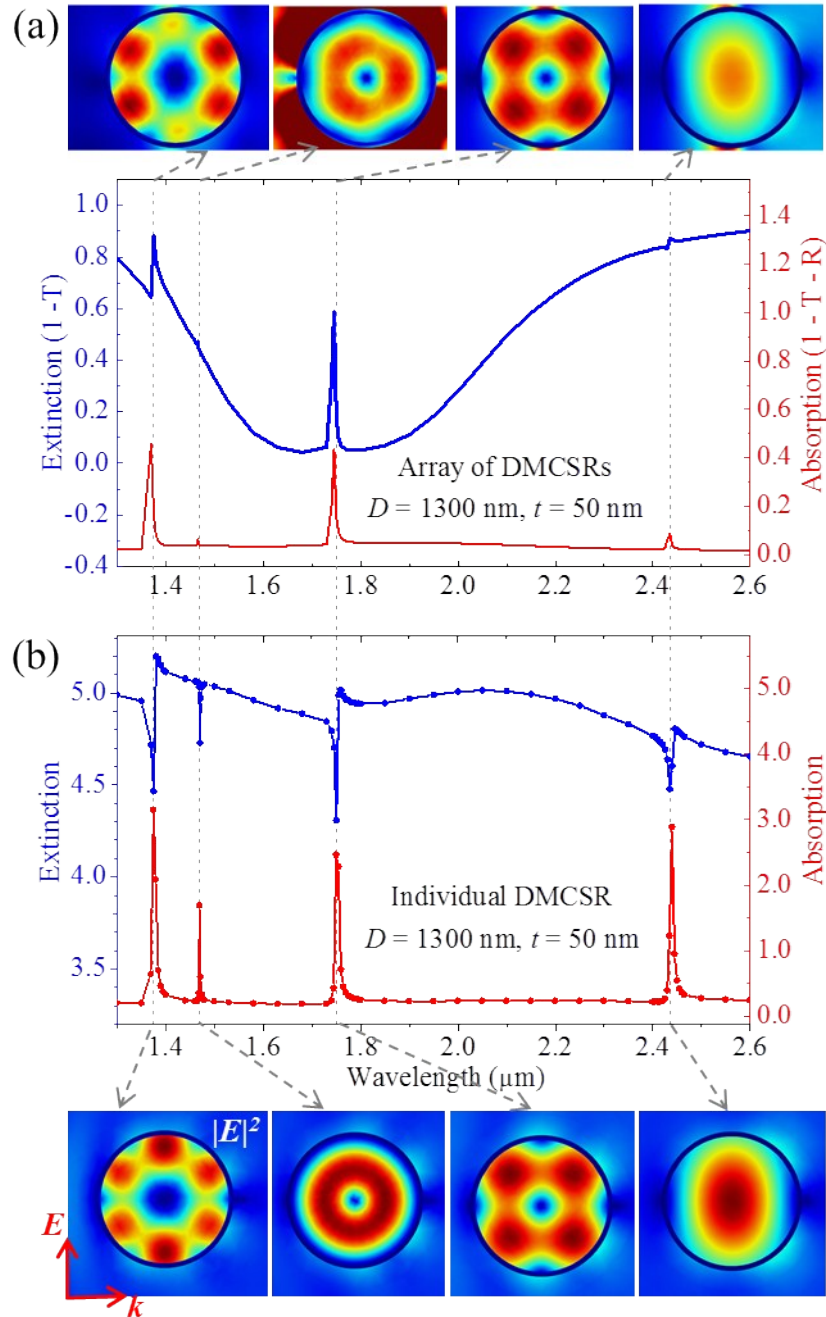


Fig. SI-2 (a) Extinction (blue curve) and absorption (red curve) spectra calculated at normal incidence for an array of DMCSRs. (b) Extinction (blue curve) and absorption (red curve) spectra calculated for an individual DMCSR. The insets show the electric field intensity distributions calculated at resonance wavelengths. In (a) and (b), the PS core diameter is $D = 1300$ nm, the thickness of the silver shell is $t = 50$ nm, and the calculations are performed in COMSOL Multiphysics. It is seen that the resonance positions and the field distributions within the dielectric core at the cavity plasmons in the array of DMCSRs are almost the same as that in the individual DMCSR.

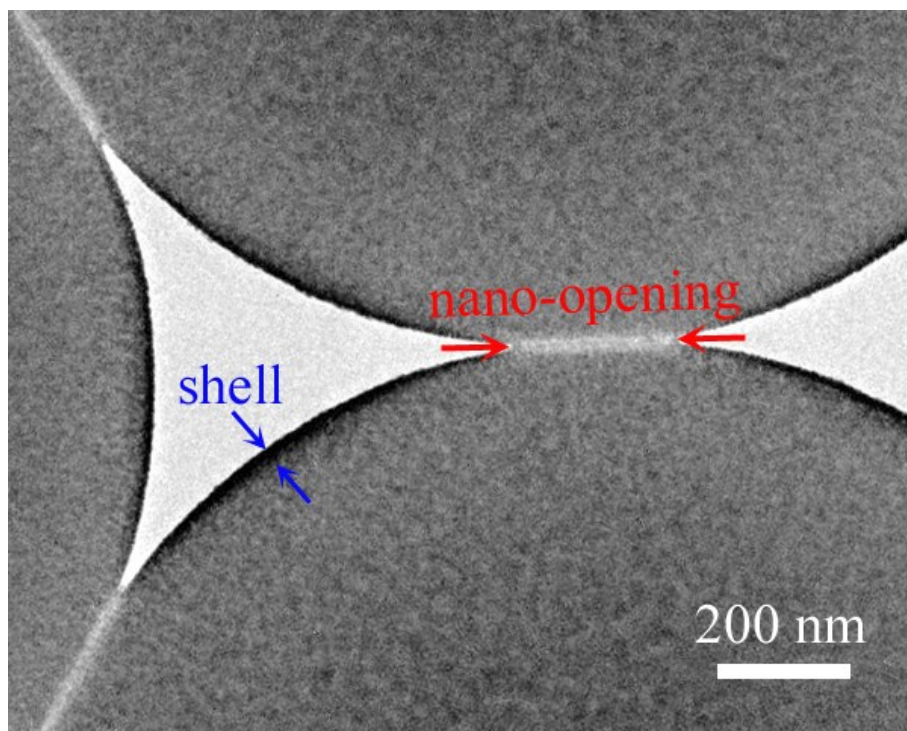


Fig. SI-3 TEM image of the prepared DMCSRs with a small shell thickness of $t \sim 12$ nm. Due to the direct contact between adjacent dielectric spheres, the silver film cannot be fully deposited onto those contact areas, leading to nano-windows with a relatively small cone angle of $\sim 20^\circ$ in each of the prepared DMCSRs, as marked by red arrows.

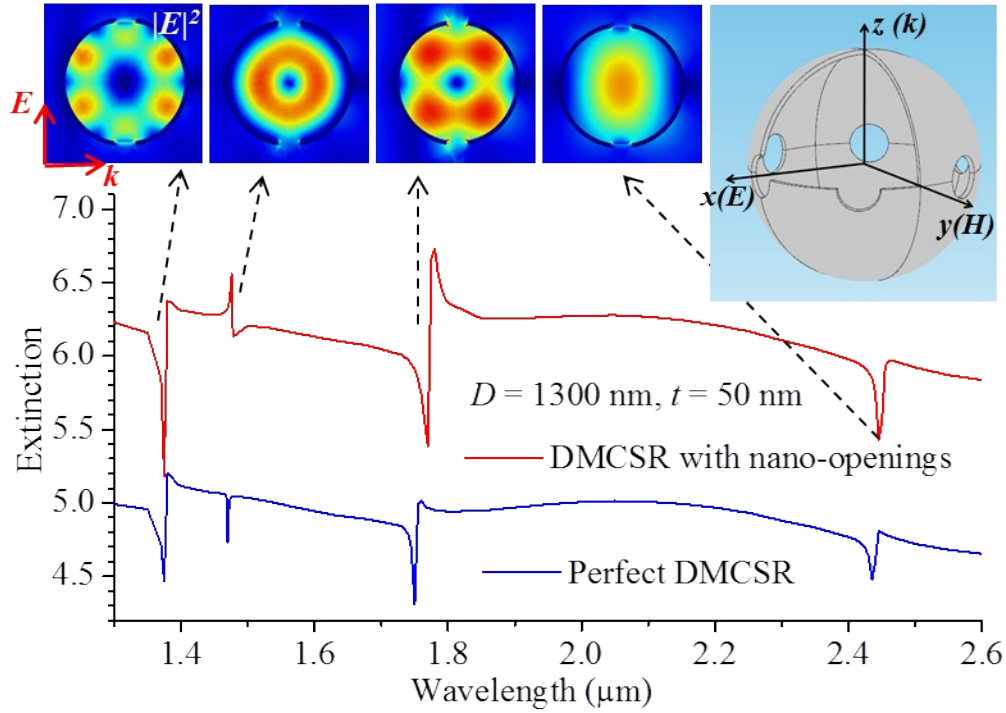


Fig. SI-4 Comparison of the extinction spectra of a perfect DMCSR with a complete metal shell layer (blue curve) and a non-perfect DMCSR having six small nano-windows with a small cone angle of 20° (red curve). The PS core diameter is $D = 1300 \text{ nm}$, the thickness of the silver shell is $t = 50 \text{ nm}$, and the calculations are performed in COMSOL Multiphysics. It is seen that compared to the perfect DMCSR, the resonance positions of the cavity plasmons are only slightly shifted for the non-perfect DMCSR with small openings. Furthermore, the insets show the electric field intensity distributions calculated at resonance wavelengths for the non-perfect DMCSR with small openings, which are almost the same as that in the perfect DMCSR shown in Fig. SI-2(b).

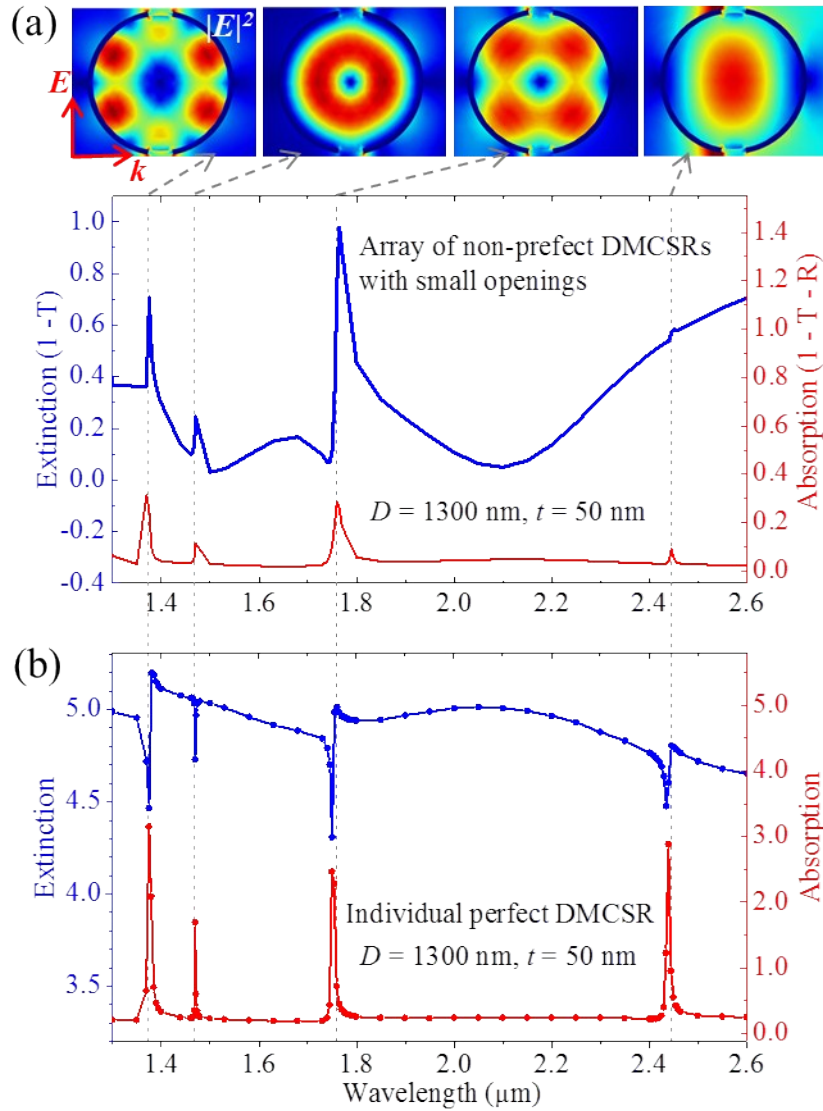


Fig. SI-5 (a) Extinction (blue curve) and absorption (red curve) spectra calculated at normal incidence for an array of non-perfect DMCSRs having six small nano-windows with a small cone angle of 20° . The insets show the electric field intensity distributions calculated at resonance wavelengths. (b) Extinction (blue curve) and absorption (red curve) spectra calculated for an individual perfect DMCSR. In (a) and (b), the PS core diameter is $D = 1300$ nm, the thickness of the silver shell is $t = 50$ nm, and the calculations are performed in COMSOL Multiphysics. It is seen that compared to the individual perfect DMCSR, the resonance positions of the cavity plasmons are only slightly shifted for the array of non-perfect DMCSR with small openings. Furthermore, the field distributions within the dielectric core at the cavity plasmons in the array of non-perfect DMCSRs are almost the same as that in the individual perfect DMCSR shown in Fig. SI-2(b).